International Journal of Medical, Medicine and Health Sciences
ISSN: 2517-9969
Vol:3, No:10, 2009

A Numerical Investigation on the Dynamic Stall of a Wind Turbine Section Using Different Turbulent Models

S. A. Ahmadi, S. Sharif, R. Jamshidi

***Abstract*—**In this article, the flow behavior around a NACA 0012 airfoil which is oscillating with different Reynolds numbers and in various amplitudes has been investigated numerically. Numerical simulations have been performed with ANSYS software. First, the 2-D geometry has been studied in different Reynolds numbers and angles of attack with various numerical methods in its static condition. This analysis was to choose the best turbulent model and comparing the grids to have the optimum one for dynamic simulations. Because the analysis was to study the blades of wind turbines, the Reynolds numbers were not arbitrary. They were in the range of 9.71e5 to 22.65e5. The angle of attack was in the range of -41.81^o to 41.81^o. By choosing the forward wind speed as the independent parameter, the others like Reynolds and the amplitude of the oscillation would be known automatically. The results show that the SST turbulent model is the best choice that leads the least numerical error with respect the experimental ones. Also, a dynamic stall phenomenon is more probable at lower wind speeds in which the lift force is less.

***Keywords*—**Dynamic stall, Numerical simulation, Wind turbine, Turbulent Model

I. Introduction

THE shedding of leading edge eddies is prominent feature of dynamic stall and is responsible for the anomalous aerodynamic force and moment encountered by an oscillating airfoil.

For an airfoil oscillating around large angle of attack, the flow separates during part of the cycle and attaches during the other part of the cycle. An interesting point is that the lift does not decrease; rather it increases in the early phase of the separation. Flow visualization [1] on 2-D airfoils show that a large vortex develops near the leading edge when the flow separates. Afterwards, the vortex convects downstream. The airfoil then experiences a sharp decrease in the lift and an increase in the drag at the moment [2]. The behavior of the vortex on 3-D wings [3] is
very different from that on 2-D airfoils. The vortex does not convect with the free stream; rather it undergoes a grow-decay cycle.

S. A. Ahmadi, M.Sc engineer, TU Clausthal, Germany
(e-mail:Ali12ir2002@yahoo.com)
S. Sharif, M.Sc engineer, Iran Uni. of Sci. and Tech., Tehran, Iran.
(e-mail: Saeedeh.sharif2007@gmail.com).
R. Jamshidi, M.Sc engineer, Sharif Uni. of Tech., Tehran, Iran
(Corresponding author to provide phone: +98-021-88328025;
e-mail: Rashid.jamshidi2009@Gmail.com).

The pressure loading are strongly affected by the mode of motion of the wings, pitching, plunging and translation [4,5] because of the deformation and convection of the separation vortex response to the instantaneous position and the history of the solid body. In an experiment, in order to know the resultant forces produced by the deterministic structure of the vortex at each instant, the surface pressure fluctuations need to be sampled and phase averaged at a large number of measuring stations at the same moment [6].

Here, a wide range of numerical modeling of an oscillating airfoil around large angles of attacks has been done. The chosen airfoil is the symmetric NACA 0012.

II. Reynolds Number

Because the relative velocity is a function of oncoming wind speed, so the Reynolds number, in which the airfoil should be analyzed, is not arbitrary. The nondimensional velocity ratio λ can be defined as the ratio of the wind turbine blade tip velocity to the oncoming wind speed:

$$\lambda = \frac{R\omega}{U_\infty} \tag{1}$$

In which, R is the radius of the rotation, ω is the angular velocity of the turbine and U_∞ is the free stream velocity. Also, the reduced frequency k can be defined as:

$$k = \frac{\lambda}{2}\frac{c}{R} \tag{2}$$

Here, c is the chord length of the cross section. By choosing a constant value for R as 1.73m, the wind speed as 10 m/s and a chord length as unity, the velocity ratio determines the Reynolds number. Here, three different values as 1.5, 2.5 and 3.5 are chosen for λ. So the amounts of k will be 0.433, 0.723 and 1.011 and the angular velocities will be 8.67, 14.45 and 20.23 in rad/sec, respectively. Because of the rotation of the blades around a vertical axis, the angle of attack changes in each period. This variation has a sinusoidal form around a zero angle of attach as below:

$$\alpha(t) = \alpha_{\max} \sin(\omega t) \tag{3}$$

In which $\alpha(t)$ is the time varying angle of attack. Also, the functionality of this value with respect to the others is as:

$$\tan(\alpha(t)) = \frac{U_\infty \sin(\varphi)}{R\omega + U_\infty \cos(\varphi)} \quad (4)$$

Here, φ is the angle of rotation of the blade. The variation of $\alpha(t)$ with respect to φ is shown in figure 1:

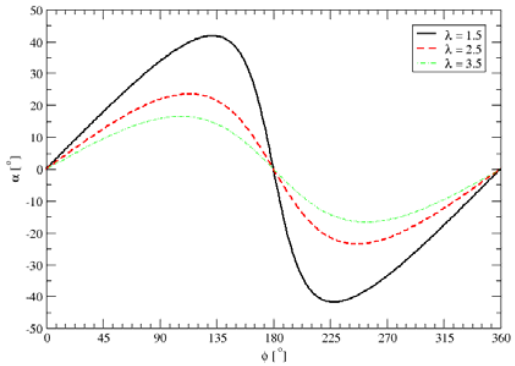

Fig. 1 Variation of α vs. φ

The maximum amplitude of oscillation is a function of the other parameters from equation (4). Table 1 shows the required parameters to compare the flow behavior in three cases:

TABLE I
VALUES REQUIRED FOR NUMERICAL SIMULATIONS

	$\lambda = 1.5$	$\lambda = 2.5$	$\lambda = 3.5$
k	0.433	0.723	1.011
α_{max}	41.81	23.57	16.6
ω	8.67	14.45	20.23
Re	9.71e5	16.18e5	22.65e5

III. GEOMETRY AND MODELING

The geometry used in this article is the famous NACA 0012 airfoil. The first step was to find out the best turbulence model for numerical simulation. This task was done by modeling a steady flow passing the stationary airfoil. The 2D model has been created in ANSYS software and a structured grid with 107000 quad elements was located in it. The inner part of the domain with 47000 elements can rotate in the dynamic model while the outer part with 60000 elements will remain stationary. The dimensions of the numerical domain and the mesh are shown in figures 2 and 3. The O type structured grid helps the solution convergence in the case of dynamic simulation and also the more precise results for static modeling.

For both static and dynamic models, the inlet boundary condition was velocity inlet in which the free stream velocity of 10 m/s was assumed. Also the upper and lower boundaries were supposed as symmetry. This indicates the normal gradient of pressure and velocity at their location is zero. The exit boundary is set as pressure outlet in which the atmospheric pressure was set.

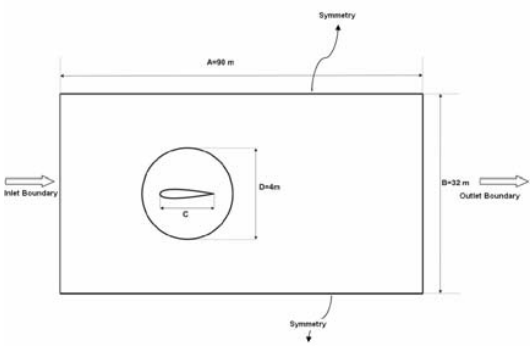

Fig. 2 Dimensions of the numerical domain

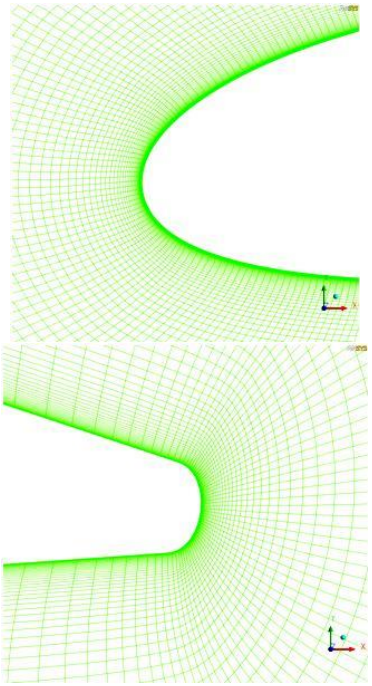

Fig. 3 Structured grids around NACA 0012 airfoil. Top: leading edge, Bottom: trailing edge

IV. STATIC MODELING

Here, the main goal is finding the best turbulence model. So, various models located in ANSYS software are examined to be compared with experimental results [7]. The examined models are: Spalart- Allmaras, SST, LLR, k-ω and SST γ-θ. The best choice would be the one with better compatibility with experimental results, both in lift and drag coefficients. The incompressible air flow passing the airfoil has Reynolds number of 3e6. Variations of drag and lift coefficients versus angle of attack are shown in figures 4 and 5.

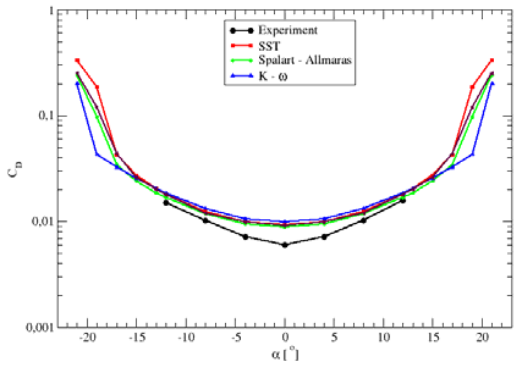

Fig. 4 Variation of drag coefficient vs. α

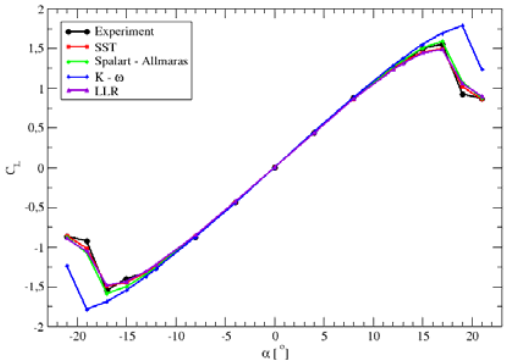

Fig. 5 Variation of lift coefficient vs. α

All of these turbulence models have some problems with viscous drag and boundary layer modeling. Conversely, their behavior in pressure field simulation is admirable. So, at lower angles of attack in which the viscous drag is more predominant the difference among experimental and numerical results is more. By increasing the angle of attack when pressure drag is very higher than viscous one, all of the models predict a value near the experiment result. Also, from figure 4, it seems that the behavior of k-ω model at high angles of attack, recede the other numerical models and can be neglected. Figure 5 Shows that k-ω has the similar problem in predicting the lift force; so this model can be omitted. Also, from the lift coefficient comparison, it's concluded that the behavior of SST model is the most similar one to the experimental data. It seems that at higher angles of attack, SST model has the nearest result to the experiment. At the stall region, that is going to be investigated here in its dynamic mode and in which vortices are the most important phenomenon that affects the dynamic stall, this model is the best choice among the others. Near zero angle of attack, all of the models predict the same behavior of the pressure and velocity field and the same lift and drag coefficients. So because of the importance of the stall region here, the SST model is chosen.

V. Dynamic Modeling: Results And Discussions

The dynamic behavior of NACA 0012 is investigated in this section at the condition of table 1. Oscillation is around zero angle of attack. Figure 6 shows the oscillatory behavior of the flow field passing the airfoil. Here, T is the period of oscillation and C_L is the lift coefficient. The net lift force on the airfoil which is perpendicular to its axis at each angle, in the last four period of oscillation, is repeating exactly the same behavior at each angle. This means that the pressure force acting on the airfoil is repetitious and also at negative angles of attack, exactly has the negative value of the corresponding positive angle of attack.

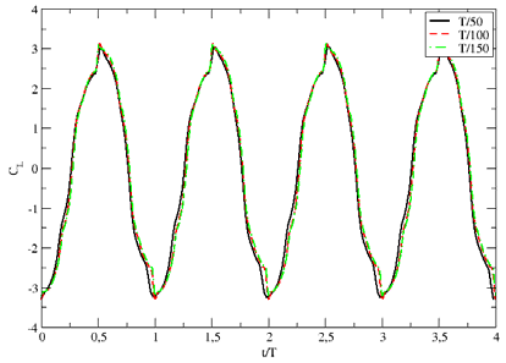

Fig. 6 Variation of lift coefficient in the last four periods vs. time

The symmetry of the behavior of NACA 0012 in oscillations can be concluded from the lift and drag graphs. For example, in figure 7 the lift coefficient versus angle of attack is drawn for $\lambda = 2.5$ in which the dotted points show different times in half of one oscillation.

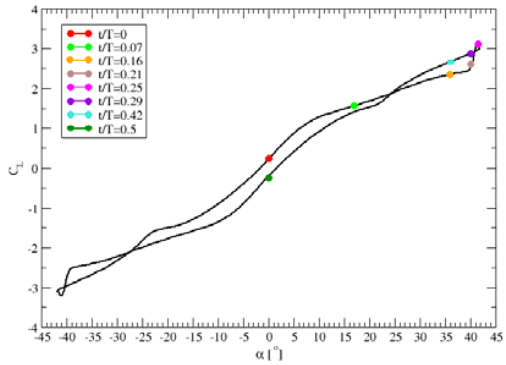

Fig. 7 Variation of lift coefficient vs. α for $\lambda = 2.5$

It can be seen that there is no dynamic stall at the maximum angle of attack. Here, because the relative velocity between

the wind and the blade is quite high and also the airfoil is symmetric, the dynamic stall phenomenon does not happen. During the one- fourth in which the airfoil is going to its maximum angle, the lift coefficient rises and at the end there is a sharp slop in its curve. This is because of generation of a wake with high velocity and low pressure from top of the airfoil at its leading edge. During the return period, this wake is being washed from the upper surface, so until a specific angle (between 25^o and 30^o), the pressure of the upper side in each angle, is less than its value at the same angle in the first one-fourth. So the lift coefficient in this interval (between 25^o and 30^o) at each specific angle in return is more than its value at the time of climbing. This can be seen by comparing the C_L at two values of t/T as 0.16 and 0.42. A similar behavior can be seen at negative angles of attack in the symmetric graph of figure 7.

For further comparison between static and dynamic responses, the lift coefficient variation versus angle of attack for three different Reynolds numbers and k numbers (equation 2) in dynamic mode and the static curve of NACA 0012 is shown in figure 8. Although there is a stall in the static curve at 17^o, but there is no sudden decrease in C_L in the dynamic curve even until 42^o. This is the main difference between dynamic and static stall. The hysteric behavior of the wakes around an oscillating airfoil that causes different phenomena in a specific angle during climbing and descending and also their time consuming motion on the upper surface of the airfoil, cause a bigger lift force for an oscillating blade. The generated wakes has their important effects during the return time to zero. Always there is a time needed to wash them from the upper surface; so the lift coefficients in a specific angle should not be equal in climbing and descending. This difference is shown for some angles during climbing and descending in figure 9.

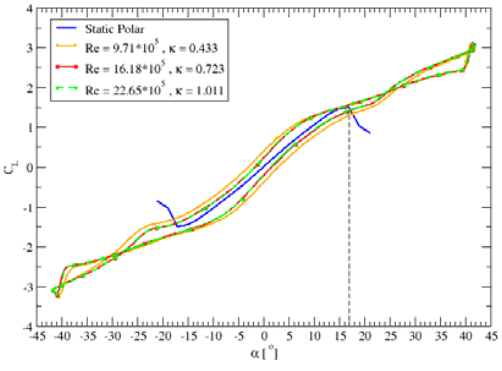

Fig. 8 Variation of lift coefficient vs. α (all with the amplitude of 41.81^o)

For vertical axis wind turbines, higher Reynolds number cause less amount of angle of attack (table 1). figures 10 and 11 show the lift coefficient hysteric behavior for two different Reynolds number and their comparison with static curve. Here, the amplitude of the oscillation is taken from table 1. Also figure 11 compares two different turbulent models in one Reynolds number. Again there is no dynamic stall at higher angles of attack and it seems that its happening is very unlikely that is because of lower amplitude of the peak angle of attack (16.6^o) because of higher relative wind velocity. It's concluded that with less velocities, C_L in figure 11 is more than its value for higher velocities in figure 10 in a specific angle. This is because of the second power of velocity in the lift coefficient formula. So in higher Reynolds and k numbers, the static curve crosses the dynamic loop and conversely, at lower Reynolds and k numbers, the dynamic loop surrounds the static curve. Also, there is no difference between the two turbulence models because large differences between the upper and lower surfaces do not happen and the wakes aren't so effective to make considerable differences between SST and SST γ-θ.

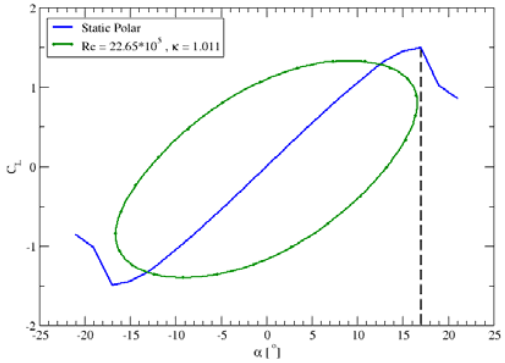

Fig. 10 Variation of lift coefficient vs. α for $\lambda = 3.5$

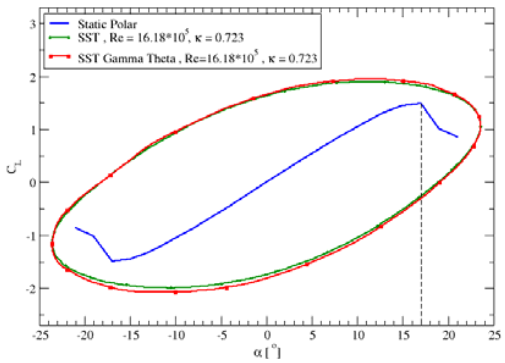

Fig. 11 Variation of lift coefficient vs. α for $\lambda = 2.5$

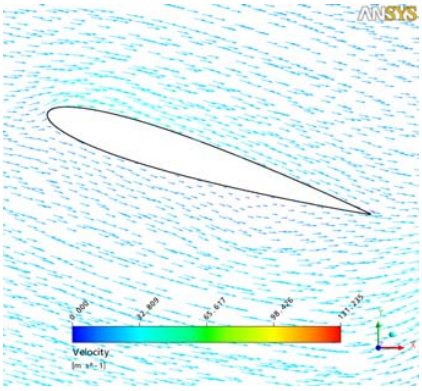

15° climbing

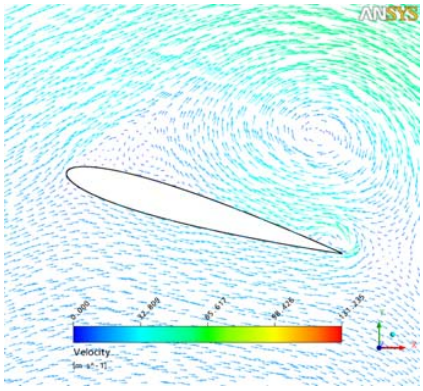

15° descending

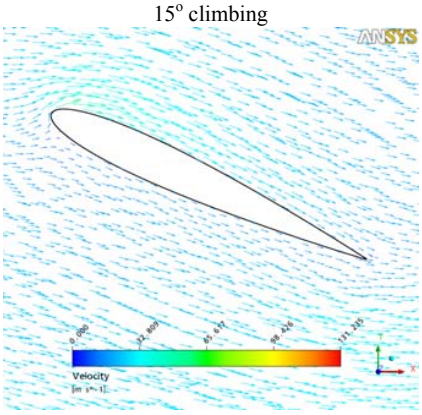

25° climbing

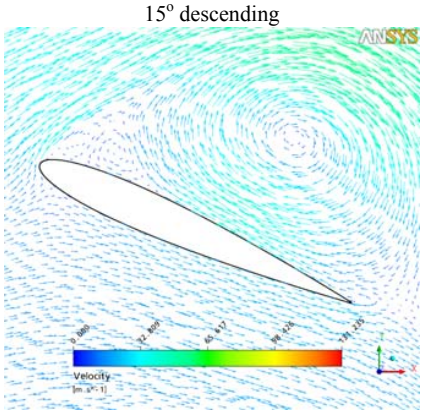

25° descending

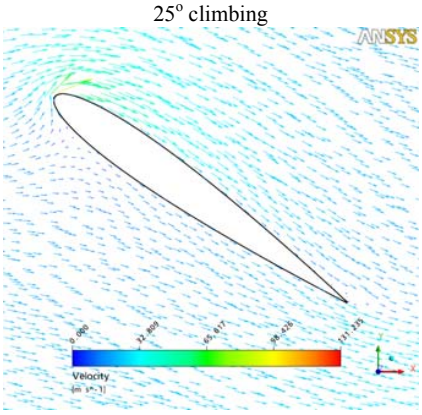

36° climbing

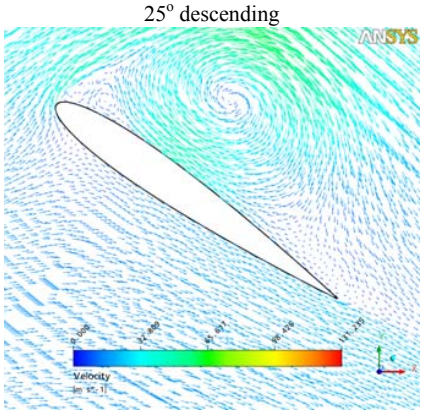

36° descending

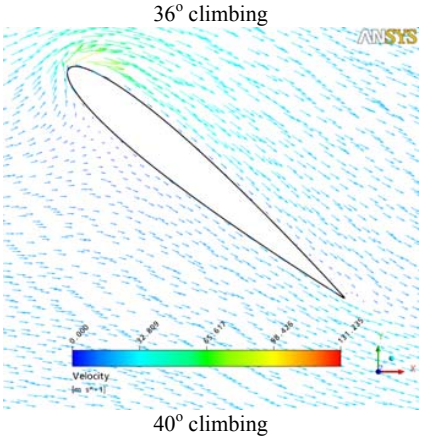

40° climbing

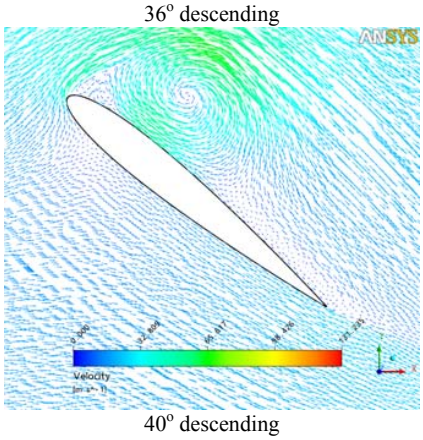

40° descending

Fig. 9 Velocity Vectors in different α s during climbing and descending

Figures 12 and 13 show the variation of C_P (pressure coefficient) on the upper and lower surfaces of the airfoil for six different times in one period of oscillation. At the earlier parts of motion (for example t/T = 0.07 and 0.16 in figure 12 and 0.21 in figure 13) the pressure of the lower and upper side of the airfoil has a smooth behavior without any local maximum or minimum but when the airfoil reaches to the peak of its amplitude (t/T= 0.25 in figure 13), the generated wakes on the upper side of it show their effects. A sudden decrease in the pressure of the upper side (in should be denoted that in figures 12 and 13, negative C_P is located upper than zero of the axis) because of the high speed wake happens and at this time this pressure jump is located at x/l=0.15 from the leading edge. After a while when the airfoil is coming down, this wake moves downstream and the location of the pressure jump at t/T = 0.29 would be at x/l = 0.35. Also at this time the wake is weaker and this is the reason of the maximum lift at the maximum angle of attack in t/T = 0.25 and less lift coefficient in t/T = 0.29 in figure 7. This behavior continues to t/T=0.42 in figure 12 in which the location of the pressure jump reaches x/l = 0.45 and it's a little weaker than x/l = 0.35. Obviously, these figures are showing the washing process of the main wake of the upper side of the airfoil that causes more lift force at higher angles of attack in dynamic motion that wouldn't happen at the same angles in a stationary airfoil.

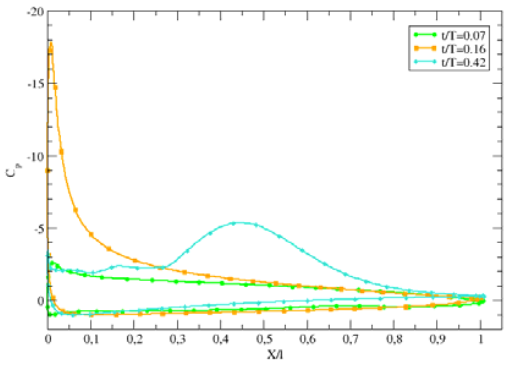

Fig. 12 Variation of pressure coefficient vs. α for $\lambda = 2.5$

Figure 14 shows the variation of drag coefficient versus angle of attack at three Reynolds and k numbers. Again all of the models are taken to the maximum amplitude of the first one, i.e. 41.81°. The symmetry of the graph for positive and negative angles show that for a symmetric airfoil, flow behavior is exactly the same for two angles equal in magnitude and negative in sign. The sudden jump of the drag coefficient near the peak (around 39°) is because of separation of the flow on the upper side exactly behind the leading edge. In figure 15, this graph is drawn again; but here for each Reynolds number, the analysis is done with its specified amplitude of table 1. It's seen that the minimum drag is not at zero angle of attack for NACA 0012. This is because of history of the wakes that affect the dynamic motion that again wouldn't happen for a stationary airfoil at zero angle of attack.

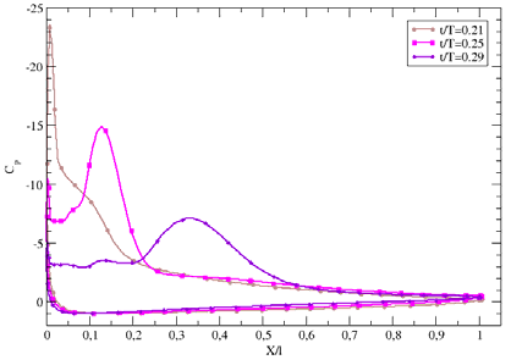

Fig. 13 Variation of lift coefficient vs. α for $\lambda = 2.5$

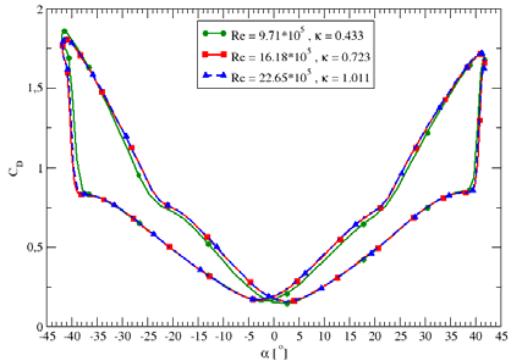

Fig. 14 Variation of drag coefficient vs. α (all with the amplitude of 41.81°)

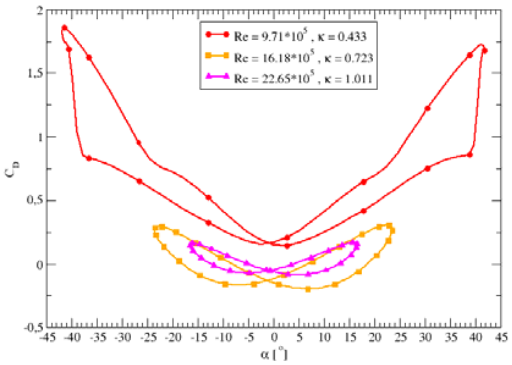

Fig. 15 Variation of drag coefficient vs. α (for each Reynolds with its specified amplitude)

VI. Conclusion

In this article, dynamic behavior of a NACA 0012 airfoil which has a pitching motion in different Reynolds numbers and in various amplitudes has been investigated numerically. By studying the stationary airfoil in different angles if attack, it's concluded that for this type of numerical simulations, the SST model without transition is the best choice that makes a good compromise in both lift and drag prediction. This model was used as the turbulence model for dynamic simulations. The analyses were done for three different Reynolds number and because they were performed for the blades of wind turbines, the Reynolds numbers were not arbitrary. They were in the range of 9.71e5 to 22.65e6. The angles of attack were in the range of -41.81^{o} to 41.81^{o}. By choosing the forward wind speed as the independent parameters, the others like Reynolds and the amplitude of the oscillation would be known automatically. The results show that the SST turbulent model is the best choice that leads the least numerical error with respect the experimental ones. Also, for this symmetric airfoil, the dynamic stall phenomenon does not happen at these case studies. the results show that the hysteric behavior of the wakes during the descending one-fourth cause different lift and drag forces with the climbing one- fourth at the same angle. These wakes need a time to wash away from the upper surface of the blade at the descending time and at this time the pressure of the upper side is less than the climbing time; so the lift would be more. This behavior repeats for each of the one-fourth and so the graphs of the lift and drag coefficients are symmetric.

References

[1] McAlister, K.W. & Carr, L.W., "Water Tunnel Visualization of Dynamic Stall", in Nonsteady Fluid Mechanics, ed. Crow, D.E. & Miller, J.A., 103-110, 1978.
[2] McCroskey W.J., "Unsteady Airfoils" Ann. Rev. of Fluid Mech., vol. 14, 285-311, 1982.
[3] Gad-el-Hak, M. & Ho, C.M., "Unsteady Vortical Flow around Three-dimensional Lifting Surfaces", to appear AIAA J., 1985.
[4] Carta, F.O., "A Comparison of the Pitching and Plunging Response of an Oscillating Airfoil", NASA CR-3172, 1979.
[5] Chen, S.H., "The Unsteady Aerodynamics of a plunging Airfoil", Ph.D. Thesis, University of Southern California, Los Angeles, California, 1985.
[6] P.B. Martin & K.W. McAlister & M.S.Chandrasekhara & W. Geissler, "Dynamic Stall Measurements and Computations for a VR-12 Airfoil with a Variable Droop Leading Edge".
[7] ANSYS software, User Manual, 2007.